Supplement of Atmos. Chem. Phys., 26, 10751–10765, 2026
https://doi.org/10.5194/acp-26-10751-2026-supplement

Atmospheric Chemistry and Physics
Open Access
EGU

Supplement of

Secondary processes driven by multi-factor interactions dominate the aerosol nitroaromatic compound pollution during winter in China

Yu Xu et al.

Correspondence to: Hao Xiao (xiaohao@sjtu.edu.cn)

Contents of the file

Texts S1–S3

Tables S1–S5

Figures S1–S7

S1. Site Description

All sampling sites in the investigated cities were located on the rooftops of 4- to 6-story buildings, either within or adjacent to university or research institute campuses. In addition, all sites were situated in urban areas with free of nearby point pollution sources such as factories, power plants, waste incineration plant, or farmland, ensuring the representativeness of regional urban atmosphere. In particular, none of the selected buildings were close to major urban arterial roads. Thus, although the urban sampling sites may be subject to the regional transport of traffic-related pollutants, the aerosol samples collected herein are not representative of ambient environments under direct, high-intensity influence from local traffic emission sources. Detailed information on all sampling sites (**Figure S1**) was shown as follows. The sampling site in Taiyuan was located at the Wucheng Campus of Shanxi University, approximately 6.5 km from the Dongshan Wulong Suburban Forest Park. The sampling site in Harbin was situated in Nangang District, adjacent to the Harbin Institute of Technology. The sampling site in Xi'an was set at the Xingqing Campus of Xi'an Jiaotong University. The sampling site in Lanzhou was located in Anning District, near Lanzhou Jiaotong University. The sampling site in Beijing was situated in a typical urban area near the Chinese Research Academy of Environmental Sciences, approximately 1–2 km from the Olympic Forest Park. The sampling site in Chengdu was located at Chengdu University of Technology in Chenghua District. The sampling site in Kunming was set at the Lianhua Campus of Kunming University of Science and Technology. The sampling site in Wuhan was located at the Wuhan Branch of the Chinese Academy of Sciences in Wuchang District.

The sampling site in Hangzhou was situated at the Zhaohui Campus of Zhejiang University of Technology, approximately 3.5 km from the West Lake Scenic Area. The sampling site in Guangzhou was located near the South China Botanical Garden, Chinese Academy of Sciences, midway between the Baiyun Mountain Scenic Area and Huolu Mountain Forest Park. The sampling site in Guiyang was situated at the Institute of Geochemistry, Chinese Academy of Sciences in Guanshanhu District, with the Yueshan Lake Wetland Park within a 2 km radius of the site.

Meteorological parameters and ambient air pollutant data were obtained from the nearest environment monitoring stations to each sampling site. As detailed previously, all sampling sites in this study were located in urban areas free of local point pollution sources. Thus, although data from these monitoring stations cannot fully capture the exact spatial average of meteorological parameters and pollutant concentrations at the sampling locations, the temporal dynamics (i.e., time-series variation trends) of the obtained data were representative of those at the sampling sites. This supports the reliability of the results derived from the correlation analysis conducted in this study.

S2. Predictions of aerosol liquid water (ALW) and pH

ALW concentration and aerosol pH were predicted using the ISORROPIA-II thermodynamic model, which has been extensively validated for the calculation of such parameters (Nguyen et al., 2016; He et al., 2018; You et al., 2026; Xu et al., 2023). This model is applicable across a broad range of ambient conditions, including relative humidity (RH) > 20% and typical tropospheric temperatures (Guo et al., 2015; Ding et al., 2019; Yang et al., 2024; Fountoukis and Nenes, 2007; Nguyen et al., 2014). The model simulations were run in forward mode under the assumption of a thermodynamically metastable state, with input datasets including particle-phase inorganic ion concentrations, ambient air temperature, and RH. The methodological details are available in our previous studies (Xu et al., 2020; Yang et al., 2024). It should be noted that the contribution of aerosol organic components to ALW was not considered in this study, as it is likely relatively minor compared to ALW derived from inorganic aerosol components (Xu et al., 2020; Nguyen et al., 2016; Xu et al., 2023).

Aerosol pH was also derived from ISORROPIA-II outputs. Specifically, the pH was predicted by considering both the equilibrium particle hydronium ion concentration per volume air (H^{+}_{air}) and the predicted inorganics-derived water (W_i), which was detailed below (Guo et al., 2015).

$$pH = -\log_{10} H_{aq}^{+} = -\log_{10} \frac{1000 H^{+}_{air}}{W_i} \quad \text{(S1)}$$

where both H^{+}_{air} and W_i were direct outputs from the ISORROPIA-II simulations. H^{+}_{aq} (mol L^{-1}) represents the hydronium ion concentration in the aqueous aerosol phase. H_{aq}^{+} value is estimated by dividing H^{+}_{air} by the ALW concentration.

A critical methodological constraint was addressed during pH calculation, which was detailed below. When ISORROPIA-II is run in forward mode with exclusive particle-phase composition inputs, it simulates the equilibrium gas-particle partitioning of NH_4^{+}. This process results in a portion of particle-phase NH_4^{+} partitioning to the gas phase as NH_3, lowering the effective particulate NH_4^+ concentration (Ding et al., 2019; Song et al., 2018). This may introduce a systematic underestimation of aerosol pH, with prior study documenting a bias of ~1 pH unit when gas-phase NH_3 measurements are unavailable as model inputs (Guo et al., 2015; Wang et al., 2021). However, it is important to note that our correlation analysis was designed to explore the synchronous temporal co-variation trends between parameters, rather than their absolute value fluctuations. Thus, the adopted ALW and pH prediction framework does not undermine the robustness or reliability of our correlation analysis results.

S3. Prediction of hydroxyl radical (·OH) concentrations

The concentrations of ·OH were estimated in this study using a widely validated empirical parameterization developed by Ehhalt and Rohrer (2000), as defined below.

$$[\cdot OH] = 4.1 \times 10^9 \times (J_{NO2})^{0.19} \times (J_{O^1D})^{0.83} \times \frac{140[NO_2]+1}{0.41[NO_2]^2+1.7[NO_2]+1} \quad (S2)$$

where J_{NO2} and J_{O^1D} denote the photolysis rate coefficients of nitrogen dioxide (NO_2) and ozone (O_3), respectively. These photolysis rate coefficients were simulated using the Tropospheric Ultraviolet and Visible (TUV) Radiation Model, accessed via the official interactive web (https://www.acom.ucar.edu/Models/TUV/Interactive_TUV/). Other required input parameters for the model simulations, including aerosol optical depth (AOD), cloud optical depth (COD), aerosol single scattering albedo (SSA), Ångström exponent (AE), cloud top height, and O_3 column concentration, were derived from the Moderate Resolution Imaging Spectroradiometer (MODIS) Level-3 daily gridded (1° × 1°) dataset (MOD08_D3/MYD08_D3). To better represent diurnal variations across sampling days, the data from Terra (morning) and Aqua (afternoon) satellites were combined and averaged. A constant surface albedo of 0.2 was prescribed for simulations. Hourly NO_2 concentration data were obtained from the official national air quality monitoring network operated by the China National Environmental Monitoring Center (http://www.cnemc.cn/).

We acknowledge that inherent uncertainties exist in our ·OH predictions, primarily driven by the complexity of tropospheric ·OH chemistry, which involves numerous interconnected production and loss pathways beyond those captured by the empirical parameterization (Vaughan et al., 2012). Nevertheless, the predicted ·OH levels remain broadly within the same order of magnitude as the measured ambient ·OH levels (Yan et al., 2019; Li et al., 2018; Hofzumahaus et al., 2009; Wang et al., 2020; Yin et al., 2026). Accordingly, these validations confirm that our predicted ·OH concentrations are broadly representative of ambient levels in the study regions. Critically, even if uncertainties remain in the absolute concentration values of ·OH, the temporal dynamics and variation trends of the predicted ·OH dataset are robust and reliably reflect those of ambient ·OH levels, which is the focus of our correlation analysis.

Table S1. Mean values (± SD) of various parameters observed in different periods and locations.

Parameter	Northern cities in China								
	HEB			TY			XA		
	Average (n = 12) Dec. 17, 2017 to Jan. 14, 2018	Clean period (n = 7)	Poll. Period (n = 5)	Average (n = 12) Dec. 10, 2017 to Jan. 8, 2018	Clean period (n = 7)	Poll. Period (n = 5)	Average (n = 12) Dec. 8, 2017 to Jan. 9, 2018	Clean period (n = 7)	Poll. Period (n = 6)
T (℃)	-17.27 ± 5.42	-17.04 ± 7.2	-17.58 ± 1.62	-2.56 ± 2.14	-3 ± 2.69	-1.95 ± 0.95	1.69 ± 2.24	1.91 ± 2.36	1.39 ± 2.28
RH (%)	66.16 ± 6.15	63.84 ± 4.52	69.4 ± 7.12	42.74 ± 8.78	36.18 ± 3.62	51.93 ± 3.41	49.27 ± 17.47	39.3 ± 7.78	63.23 ± 18.2
ALW	31.53 ± 24.65	17.35 ± 13.66	51.39 ± 23.38	21.18 ± 21.21	7.5 ± 5.98	40.33 ± 19.94	51.63 ± 81.74	7.72 ± 5.69	113.11 ± 101.13
pH	4.35 ± 1.08	3.96 ± 1.28	4.89 ± 0.35	5.99 ± 0.92	6.52 ± 0.85	5.25 ± 0.28	5.13 ± 0.90	5.36 ± 1.07	4.82 ± 0.56
SR (W m^{-2})	71.11 ± 6.34	70.27 ± 6.66	72.3 ± 6.41	119.95 ± 17.58	124.06 ± 16.06	114.2 ± 19.81	141.74 ± 31.62	159.05 ± 18.81	117.51 ± 30.98
PBLH (m)	339.03 ± 191.45	457.34 ± 162.41	173.40 ± 49.43	410.47 ± 361.30	600.59 ± 368.43	144.30 ± 59.63	166.74 ± 67.59	176.70 ± 84.45	152.80 ± 38.10
·OH (×10^5 molecule cm^{-3})	3.05 ± 1.25	3.54 ± 1.23	2.35 ± 1.00	3.00 ± 2.14	4.27 ± 1.96	1.22 ± 0.31	1.70 ± 1.14	2.42 ± 0.86	0.68 ± 0.51
SO_2 (μg m^{-3})	56.24 ± 18.84	44.45 ± 10.23	72.75 ± 15.34	60.36 ± 40.28	31.62 ± 23.46	100.6 ± 12.94	31.73 ± 12.13	24.15 ± 5.08	42.34 ± 11.16
$PM_{2.5}$ (μg m^{-3})	90.62 ± 65.15	45.31 ± 18.11	154.04 ± 50.60	81.02 ± 65.20	33.58 ± 20.46	147.45 ± 40.08	115.33 ± 88.85	52.45 ± 16.8	203.37 ± 68.42
O_3 (μg m^{-3})	37.84 ± 10.47	43.88 ± 8.21	29.38 ± 6.86	30.07 ± 22.84	43.57 ± 21.10	11.18 ± 1.04	24.67 ± 13.35	31.41 ± 11.8	15.23 ± 9.53
NO_3^- (μg m^{-3})	9.16 ± 6.64	7.66 ± 7.74	11.25 ± 4.68	14.95 ± 14.27	6.50 ± 2.83	26.78 ± 15.75	40.56 ± 31.79	20.89 ± 10.2	68.11 ± 31.58
SO_4^{2-} (μg m^{-3})	11.45 ± 7.34	7.26 ± 3.73	17.31 ± 7.33	16.51 ± 13.23	9.17 ± 1.35	29.36 ± 15.31	21.58 ± 17.3	11.14 ± 3.05	36.19 ± 18.75
Ca^{2+} (μg m^{-3})	0.93 ± 0.39	0.72 ± 0.30	1.23 ± 0.31	6.09 ± 1.72	5.21 ± 1.67	7.31 ± 0.85	6.69 ± 5.72	4.85 ± 1.92	9.26 ± 8.38
Mg^{2+} (μg m^{-3})	0.10 ± 0.06	0.09 ± 0.08	0.10 ± 0.03	0.34 ± 0.13	0.25 ± 0.07	0.47 ± 0.09	0.36 ± 0.36	0.21 ± 0.09	0.56 ± 0.51
NH_4^+ (μg m^{-3})	8.23 ± 5.71	5.26 ± 3.63	12.39 ± 5.72	12.11 ± 11.66	5.86 ± 1.64	20.86 ± 14.34	20.58 ± 17.78	8.79 ± 2.98	37.1 ± 16.5
nss-K^+ (μg m^{-3})	1.87 ± 1.37	1.10 ± 0.70	2.94 ± 1.39	1.19 ± 0.97	0.63 ± 0.25	1.98 ± 1.09	2.63 ± 1.99	1.63 ± 0.91	4.05 ± 2.32
nss-Cl^- (μg m^{-3})	5.19 ± 4.44	2.81 ± 2.24	8.51 ± 4.79	6.51 ± 5.60	3.49 ± 2.20	10.74 ± 6.37	6.01 ± 3.82	4.38 ± 2.10	8.3 ± 4.71
$C_8H_{17}O_4S^-$ (ng m^{-3})	0.21 ± 0.09	0.21 ± 0.12	0.20 ± 0.05	0.49 ± 0.21	0.43 ± 0.21	0.57 ± 0.20	0.49 ± 0.16	0.51 ± 0.20	0.46 ± 0.09

$C_5H_7O_6S^-$ (ng m^{-3})	17.90 ± 11.61	21.93 ± 13.51	12.27 ± 5.37	12.19 ± 3.18	12.03 ± 3.14	12.42 ± 3.59	12.75 ± 3.61	13.93 ± 4.12	11.08 ± 2.10
4NP (ng m^{-3})	10.57 ± 5.73	9.23 ± 6.74	12.46 ± 3.82	11.68 ± 2.88	11.23 ± 3.47	12.31 ± 1.97	12.77 ± 3.51	12.88 ± 4.25	12.62 ± 2.60
3M4NP (ng m^{-3})	2.96 ± 1.49	2.64 ± 1.70	3.40 ± 1.15	4.75 ± 2.22	5.67 ± 2.18	3.48 ± 1.70	2.89 ± 1.08	3.18 ± 1.29	2.47 ± 0.58
2M4NP (ng m^{-3})	3.74 ± 1.97	3.31 ± 2.31	4.34 ± 1.38	4.47 ± 2.04	5.24 ± 2.17	3.39 ± 1.35	3.39 ± 1.18	3.78 ± 1.41	2.85 ± 0.48
2,4DNP (ng m^{-3})	0.38 ± 0.20	0.35 ± 0.19	0.42 ± 0.21	2.68 ± 1.70	1.78 ± 0.86	3.95 ± 1.85	1.87 ± 1.20	1.57 ± 0.41	2.27 ± 1.83
Total NPs (ng m^{-3})	17.65 ± 9.28	15.53 ± 10.89	20.62 ± 6.34	23.59 ± 6.79	23.92 ± 8.00	23.12 ± 5.49	20.92 ± 5.64	21.42 ± 6.73	20.22 ± 4.31
4M5NC (ng m^{-3})	0.42 ± 0.31	0.32 ± 0.16	0.56 ± 0.44	0.49 ± 0.32	0.47 ± 0.33	0.51 ± 0.35	0.19 ± 0.12	0.22 ± 0.16	0.16 ± 0
4NC (ng m^{-3})	20.71 ± 7.55	17.85 ± 7.57	24.71 ± 6.02	9.84 ± 6.24	7.89 ± 3.64	12.58 ± 8.43	15.5 ± 5.50	17.15 ± 5.6	13.19 ± 4.96
Total NCs (ng m^{-3})	21.13 ± 7.55	18.17 ± 7.48	25.27 ± 6.00	10.33 ± 6.28	8.36 ± 3.82	13.09 ± 8.38	15.69 ± 5.51	17.37 ± 5.61	13.35 ± 4.96
5NSA (ng m^{-3})	0.41 ± 0.36	0.34 ± 0.43	0.51 ± 0.25	0.73 ± 0.66	0.35 ± 0.26	1.28 ± 0.68	1.08 ± 0.41	0.78 ± 0.20	1.50 ± 0.11
3NSA (ng m^{-3})	0.55 ± 0.48	0.45 ± 0.55	0.69 ± 0.38	0.67 ± 0.82	0.18 ± 0.19	1.35 ± 0.89	1.15 ± 0.77	0.55 ± 0.19	1.99 ± 0.27
Total NSAs (ng m^{-3})	0.96 ± 0.84	0.80 ± 0.97	1.20 ± 0.62	1.40 ± 1.47	0.53 ± 0.43	2.62 ± 1.57	2.23 ± 1.16	1.33 ± 0.34	3.49 ± 0.37
4NG (ng m^{-3})	5.12 ± 1.90	4.18 ± 1.80	6.43 ± 1.18	2.98 ± 1.77	2.94 ± 1.73	3.04 ± 2.03	3.29 ± 1.43	3.75 ± 1.47	2.64 ± 1.24
Total NACs (ng m^{-3})	44.87 ± 17.83	38.68 ± 19.19	53.52 ± 12.70	38.3 ± 12.2	35.75 ± 12.81	41.87 ± 11.66	42.13 ± 12.13	43.87 ± 13.64	39.7 ± 10.63

Table S2. Mean values (± SD) of various parameters observed in different periods and locations.

Parameter	Northern cities in China					
	LZ			BJ		
	Average (n = 12) Dec. 7, 2017 to Jan. 8, 2018	Clean period (n = 7)	Poll. Period (n = 5)	Average (n = 12) Dec. 10, 2017 to Jan. 14, 2018	Clean period (n = 8)	Poll. Period (n = 4)
T (℃)	-5.72 ± 2.77	-7.26 ± 2.30	-3.56 ± 1.79	-1.58 ± 2.21	-1.16 ± 2.20	-2.83 ± 2.10
RH (%)	53.85 ± 10.59	58.14 ± 11.03	47.85 ± 6.98	48.53 ± 21.71	39.59 ± 14.70	75.34 ± 17.00
ALW	20.44 ± 13.37	17.03 ± 15.84	25.22 ± 8.16	26.48 ± 42.79	9.9 0± 15.37	76.24 ± 64.6
pH	5.18 ± 0.93	4.86 ± 0.36	5.64 ± 1.33	6.31 ± 1.80	6.96 ± 1.59	4.37 ± 0.45
SR (W m^{-2})	139.16 ± 13.98	136.92 ± 18.18	142.28 ± 4.54	112.91 ± 9.06	112.31 ± 10.26	114.70 ± 4.93
PBLH (m)	273.10 ± 163.15	347.22 ± 174.53	169.32 ± 66.57	407.88 ± 327.18	466.34 ± 351.64	232.48 ± 180.68
·OH (×10^5 molecule cm^{-3})	2.22 ± 1.74	3.19 ± 1.65	0.85 ± 0.50	3.67 ± 1.84	4.41 ± 1.45	1.45 ± 0.64
SO_2 (μg m^{-3})	48.00 ± 20.40	35.77 ± 15.67	65.13 ± 12.15	6.95 ± 3.34	6.59 ± 3.24	8.04 ± 4.10
$PM_{2.5}$ (μg m^{-3})	86.37 ± 42.14	54.16 ± 14.04	131.46 ± 15.17	52.67 ± 53.71	25.99 ± 21.38	132.71 ± 35.00
O_3 (μg m^{-3})	30.36 ± 12.83	36.29 ± 14.15	22.06 ± 2.24	31.15 ± 18.29	37.24 ± 16.73	12.89 ± 7.39
NO_3^- (μg m^{-3})	19.91 ± 14.91	12.00 ± 6.59	30.99 ± 16.83	10.77 ± 15.24	4.38 ± 5.57	29.96 ± 20.43
SO_4^{2-} (μg m^{-3})	18.15 ± 11.7	11.61 ± 4.56	27.31 ± 12.87	7.40 ± 8.46	3.89 ± 3.86	17.91 ± 10.65
Ca^{2+} (μg m^{-3})	5.83 ± 3.90	4.03 ± 1.00	8.35 ± 5.18	2.33 ± 0.74	2.52 ± 0.49	1.75 ± 1.16
Mg^{2+} (μg m^{-3})	0.31 ± 0.36	0.17 ± 0.04	0.51 ± 0.51	0.15 ± 0.03	0.14 ± 0.02	0.17 ± 0.04
NH_4^+ (μg m^{-3})	10.13 ± 7.04	6.78 ± 3.08	14.82 ± 8.65	6.6 ± 9.50	2.68 ± 3.04	18.37 ± 13.50
nss-K^+ (μg m^{-3})	0.66 ± 0.41	0.39 ± 0.21	1.03 ± 0.30	0.57 ± 0.49	0.40 ± 0.32	1.08 ± 0.61
nss-Cl^- (μg m^{-3})	1.23 ± 1.14	0.83 ± 0.72	1.78 ± 1.46	2.03 ± 1.90	1.40 ± 1.17	3.92 ± 2.68
$C_8H_{17}O_4S^-$ (ng m^{-3})	0.42 ± 0.18	0.35 ± 0.19	0.52 ± 0.11	0.29 ± 0.08	0.27 ± 0.09	0.32 ± 0.05

$C_5H_7O_6S^-$ (ng m^{-3})	11.48 ± 3.79	12.43 ± 4.72	10.14 ± 1.53	9.60 ± 3.64	10.02 ± 4.14	8.34 ± 1.11
4NP (ng m^{-3})	6.53 ± 2.43	5.35 ± 1.88	8.17 ± 2.27	6.31 ± 2.32	6.35 ± 2.60	6.20 ± 1.60
3M4NP (ng m^{-3})	1.69 ± 0.47	1.60 ± 0.53	1.82 ± 0.39	2.00 ± 0.83	2.24 ± 0.80	1.26 ± 0.37
2M4NP (ng m^{-3})	1.96 ± 0.60	1.74 ± 0.57	2.27 ± 0.56	2.08 ± 0.73	2.30 ± 0.71	1.42 ± 0.11
2,4DNP (ng m^{-3})	1.76 ± 2.92	1.01 ± 0.66	2.83 ± 4.51	1.06 ± 0.63	1.18 ± 0.61	0.71 ± 0.66
Total NPs (ng m^{-3})	11.95 ± 5.13	9.70 ± 3.31	15.09 ± 5.90	11.45 ± 3.50	12.07 ± 3.87	9.59 ± 0.84
4M5NC (ng m^{-3})	0.23 ± 0.10	0.23 ± 0.09	0.23 ± 0.11	0.27 ± 0.13	0.28 ± 0.13	0.26 ± 0.12
4NC (ng m^{-3})	5.79 ± 3.70	4.72 ± 3.12	7.30 ± 4.27	4.83 ± 2.91	4.70 ± 3.31	5.22 ± 1.56
Total NCs (ng m^{-3})	6.02 ± 3.75	4.95 ± 3.19	7.53 ± 4.32	5.10 ± 2.97	4.98 ± 3.39	5.48 ± 1.54
5NSA (ng m^{-3})	0.61 ± 0.42	0.39 ± 0.25	0.92 ± 0.43	0.47 ± 0.60	0.24 ± 0.36	1.14 ± 0.76
3NSA (ng m^{-3})	0.75 ± 0.67	0.41 ± 0.35	1.24 ± 0.74	0.42 ± 0.69	0.18 ± 0.43	1.14 ± 0.91
Total NSAs (ng m^{-3})	1.36 ± 1.09	0.80 ± 0.59	2.16 ± 1.17	0.89 ± 1.28	0.42 ± 0.78	2.28 ± 1.66
4NG (ng m^{-3})	1.23 ± 0.55	1.13 ± 0.7	1.38 ± 0.24	1.25 ± 0.82	1.32 ± 0.93	1.04 ± 0.35
Total NACs (ng m^{-3})	20.56 ± 7.95	16.57 ± 7.31	26.16 ± 5.18	18.69 ± 7.14	18.79 ± 8.19	18.39 ± 3.42

Table S3. Mean values (± SD) of various parameters observed in different periods and locations.

Parameter	Southern cities								
	CD			KM			WH		
	Average (n = 12) Dec. 8, 2017 to Jan. 6, 2018	Clean period (n = 6)	Poll. Period (n = 6)	Average (n = 12) Dec. 12, 2017 to Jan. 6, 2018	Clean period (n = 8)	Poll. Period (n = 4)	Average (n = 12) Dec. 11, 2017 to Jan. 8, 2018	Clean period (n = 6)	Poll. Period (n = 6)
T (°C)	5.82 ± 1.29	6.48 ± 1.19	4.90 ± 0.79	9.63 ± 2.52	9.88 ± 2.98	9.12 ± 1.42	3.89 ± 2.88	2.06 ± 2.48	5.71 ± 2.03
RH (%)	74.75 ± 7.65	71.48 ± 5.65	79.33 ± 8.26	68.25 ± 7.73	68.44 ± 8.83	67.88 ± 6.07	78.84 ± 11.53	81.94 ± 14.27	75.75 ± 8.10
ALW	65.76 ± 96.89	13.76 ± 8.73	138.57 ± 119.76	8.18 ± 6.42	5.64 ± 6.45	13.28 ± 1.42	74.42 ± 89.97	82.53 ± 116.36	66.31 ± 64.1
pH	3.51 ± 0.38	3.43 ± 0.18	3.62 ± 0.57	4.06 ± 1.61	4.33 ± 1.93	3.52 ± 0.48	3.49 ± 0.82	3.57 ± 1.16	3.41 ± 0.35
SR (W m^{-2})	138.45 ± 40.09	117.27 ± 31.56	168.1 ± 32.29	176.3 ± 54.5	176.03 ± 60.38	176.83 ± 48.83	130.02 ± 54.30	127.63 ± 50.32	132.41 ± 62.79
PBLH (m)	365.22 ± 96.81	429.01 ± 71.34	275.90 ± 32.31	451.46 ± 155.51	503.28 ± 155.05	347.82 ± 105.29	269.18 ± 104.97	328.61 ± 93.83	209.74 ± 83.4
·OH (×10^5 molecule cm^{-3})	1.96 ± 1.32	2.04 ± 1.68	1.84 ± 0.76	8.14 ± 4.44	9.52 ± 4.58	5.40 ± 2.91	3.10 ± 2.19	3.24 ± 2.59	2.96 ± 1.94
SO_2 (μg m^{-3})	10.61 ± 2.86	9.24 ± 2.73	12.53 ± 1.84	18.45 ± 5.34	17.39 ± 5.01	20.57 ± 6.08	12.84 ± 6.17	8.60 ± 6.09	17.08 ± 1.87
$PM_{2.5}$ (μg m^{-3})	85.58 ± 58.16	43.99 ± 19.78	143.79 ± 38.10	47.62 ± 30.50	28.28 ± 12.14	86.30 ± 8.63	88.54 ± 35.69	58.43 ± 16.12	118.65 ± 19.13
O_3 (μg m^{-3})	26.85 ± 9.37	29.22 ± 10.67	23.53 ± 6.85	37.55 ± 16.19	35.69 ± 12.67	41.26 ± 23.65	24.21 ± 10.39	28.83 ± 11.36	19.59 ± 7.55
NO_3^- (μg m^{-3})	20.80 ± 19.54	8.80 ± 4.18	37.60 ± 20.47	4.83 ± 3.80	3.11 ± 2.73	8.29 ± 3.42	19.13 ± 12.00	11.25 ± 10.87	27.01 ± 7.04
SO_4^{2-} (μg m^{-3})	10.35 ± 8.82	4.97 ± 1.82	17.88 ± 9.35	8.09 ± 4.53	5.71 ± 3.18	12.84 ± 2.52	9.52 ± 5.17	7.63 ± 4.99	11.42 ± 5.02
Ca^{2+} (μg m^{-3})	2.08 ± 1.20	1.85 ± 0.96	2.42 ± 1.52	2.91 ± 1.07	2.57 ± 0.83	3.59 ± 1.30	2.34 ± 1.60	1.67 ± 1.63	3.00 ± 1.37
Mg^{2+} (μg m^{-3})	0.10 ± 0.06	0.08 ± 0.04	0.14 ± 0.06	0.08 ± 0.03	0.07 ± 0.03	0.11 ± 0.02	0.11 ± 0.06	0.07 ± 0.05	0.14 ± 0.05
NH_4^+ (μg m^{-3})	10.6 ± 10.65	4.45 ± 1.89	19.21 ± 12.14	3.78 ± 2.67	2.47 ± 1.71	6.39 ± 2.36	8.83 ± 4.64	7.14 ± 3.30	10.52±5.44
nss-K^+ (μg m^{-3})	1.16 ± 0.77	0.63 ± 0.49	1.90 ± 0.28	0.53 ± 0.36	0.31 ± 0.14	0.95 ± 0.25	1.00 ± 0.61	0.51 ± 0.23	1.50 ± 0.44
nss-Cl^- (μg m^{-3})	2.58 ± 1.92	1.57 ± 1.11	3.99 ± 2.00	0.74 ± 0.38	0.63 ± 0.38	0.96 ± 0.30	1.63 ± 1.16	1.06 ± 0.63	2.21 ± 1.34
$C_8H_{17}O_4S^-$ (ng m^{-3})	0.24 ± 0.06	0.23 ± 0.06	0.26 ± 0.07	0.45 ± 0.36	0.31 ± 0.30	0.73 ± 0.33	0.25 ± 0.17	0.28 ± 0.18	0.21 ± 0.16

$C_5H_7O_6S^-$ (ng m^{-3})	6.52 ± 1.95	5.81 ± 1.81	7.50 ± 1.86	6.03 ± 2.79	5.28 ± 2.97	7.54 ± 1.87	4.92 ± 1.76	4.38 ± 1.31	5.45 ± 2.10
4NP (ng m^{-3})	5.23 ± 2.38	3.89 ± 1.93	7.10 ± 1.59	1.32 ± 0.96	1.18 ± 1.05	1.59 ± 0.84	2.60 ± 1.12	2.19 ± 0.85	3.02 ± 1.28
3M4NP (ng m^{-3})	0.65 ± 0.29	0.54 ± 0.26	0.81 ± 0.27	0.20 ± 0.22	0.26 ± 0.24	0.07 ± 0.08	0.29 ± 0.20	0.25 ± 0.19	0.32 ± 0.22
2M4NP (ng m^{-3})	1.00 ± 0.40	0.82 ± 0.34	1.25 ± 0.37	0.24 ± 0.25	0.30 ± 0.28	0.12 ± 0.14	0.42 ± 0.29	0.37 ± 0.26	0.46 ± 0.34
2,4DNP (ng m^{-3})	0.46 ± 0.30	0.52 ± 0.35	0.37 ± 0.23	0.30 ± 0.16	0.25 ± 0.17	0.41 ± 0.04	0.52 ± 0.51	0.52 ± 0.58	0.53 ± 0.49
Total NPs (ng m^{-3})	7.34 ± 3.15	5.78 ± 2.78	9.52 ± 2.35	2.05 ± 1.38	1.99 ± 1.59	2.18 ± 1.02	3.83 ± 1.88	3.33 ± 1.78	4.34 ± 2.00
4M5NC (ng m^{-3})	0.16 ± 0	0.16 ± 0	0.16 ± 0	0.26 ± 0.10	0.24 ± 0.05	0.32 ± 0.15	0.18 ± 0.07	0.15 ± 0	0.22 ± 0.09
4NC (ng m^{-3})	8.43 ± 4.88	5.73 ± 4.45	12.21 ± 2.26	3.66 ± 1.87	3.03 ± 1.96	4.92 ± 0.88	3.40 ± 2.05	2.12 ± 1.30	4.67 ± 1.90
Total NCs (ng m^{-3})	8.59 ± 4.88	5.89 ± 4.45	12.37 ± 2.26	3.93 ± 1.89	3.27 ± 1.92	5.25 ± 1.00	3.58 ± 2.08	2.26 ± 1.30	4.89 ± 1.92
5NSA (ng m^{-3})	0.78 ± 0.40	0.53 ± 0.31	1.14 ± 0.15	0.18 ± 0.24	0.07 ± 0.14	0.40± 0.28	0.55 ± 0.33	0.35 ± 0.36	0.74 ± 0.14
3NSA (ng m^{-3})	0.46 ± 0.39	0.19 ± 0.17	0.85 ± 0.23	0.04 ± 0.08	0.02 ± 0.07	0.08 ± 0.10	0.42 ± 0.26	0.32 ± 0.23	0.51 ± 0.28
Total NSAs (ng m^{-3})	1.24 ± 0.74	0.72 ± 0.43	1.98 ± 0.28	0.22 ± 0.31	0.10 ± 0.20	0.48 ± 0.35	0.97 ± 0.52	0.68 ± 0.51	1.25 ± 0.37
4NG (ng m^{-3})	1.58 ± 0.90	1.23 ± 0.89	2.08 ± 0.70	0.67 ± 0.31	0.57 ± 0.33	0.86 ± 0.17	0.52 ± 0.30	0.36 ± 0.21	0.67 ± 0.29
Total NACs (ng m^{-3})	18.75 ± 9.37	13.62 ± 8.44	25.95 ± 4.88	6.88 ± 3.58	5.93 ± 3.88	8.78 ± 2.17	8.89 ± 4.34	6.63 ± 3.66	11.16 ± 3.98

Table S4. Mean values (± SD) of various parameters observed in different periods and locations.

Parameter	Southern cities								
	HZ			GZ			GY		
	Average (n = 12) Dec. 16, 2017 to Jan. 8, 2018	Clean period (n = 6)	Poll. Period (n = 6)	Average (n = 12) Dec. 16, 2017 to Jan. 8, 2018	Clean period (n = 7)	Poll. Period (n = 5)	Average (n = 12) Dec. 14, 2017 to Jan. 7, 2018	Clean period (n = 9)	Poll. Period (n = 3)
T (°C)	6.61 ± 2.49	5.08 ± 1.62	8.74 ± 1.85	15.9 ± 3.25	14.2 ± 3.00	18.29 ± 1.85	5.58 ± 3.29	4.93 ± 3.22	8.81 ± 0.46
RH (%)	73.83 ± 17.61	76.84 ± 17.38	69.63 ± 19.03	62.04 ± 21.39	62.93 ± 28.03	60.79 ± 8.73	78.88 ± 20.50	84.34 ± 17.71	51.56 ± 2.92
ALW	64.64 ± 69.04	57.58 ± 45.20	74.52 ± 99.17	19.62 ± 25.35	21.95 ± 33.76	16.35 ± 5.84	37.64 ± 40.88	42.82 ± 43.05	11.75 ± 9.59
pH	3.37 ± 0.59	3.54 ± 0.30	3.14 ± 0.84	2.65 ± 0.76	2.96 ± 0.87	2.21 ± 0.24	3.34 ± 0.53	3.42 ± 0.53	2.97 ± 0.55
SR (W m^{-2})	128.11 ± 59.08	139.98 ± 64.14	111.49 ± 53.26	140.30 ± 61.44	149.07 ± 77.60	128.02 ± 32.02	124.02 ± 40.92	120.45 ± 38.20	141.87 ± 67.21
PBLH (m)	414.10 ± 249.60	494.17 ± 261.18	302.01 ± 205.12	404.53 ± 200.27	498.48 ± 208.57	273.01 ± 89.32	380.66 ± 182.81	373.32 ± 194.26	417.31 ± 157.42
·OH ($\times 10^5$)	1.82 ± 1.23	1.98 ± 1.47	1.60 ± 0.91	4.06 ± 3.38	4.83 ± 4.18	2.99 ± 1.66	3.98 ± 2.47	4.01 ± 2.59	3.87 ± 2.56
SO_2 (μg m^{-3})	13.12 ± 3.59	11.37 ± 2.60	15.57 ± 3.53	15.87 ± 6.29	12.54 ± 5.960	20.53 ± 2.98	43.33 ± 18.64	36.6 ± 11.06	76.98 ± 1.38
$PM_{2.5}$ (μg m^{-3})	69.12 ± 28.14	51.90 ± 20.62	93.23 ± 17.15	56.41 ± 33.06	32.13 ± 17.95	90.40 ± 6.85	49.47 ± 26.17	40.08 ± 14.71	96.44 ± 17.12
O_3 (μg m^{-3})	26.39 ± 17.90	23.68 ± 14.35	30.18 ± 23.26	34.62 ± 22.76	28.81 ± 26.40	42.75 ± 15.40	47.10 ± 31.46	38.54 ± 26.20	89.88 ± 17.80
NO_3^- (μg m^{-3})	18.91 ± 8.03	14.90 ± 7.15	24.51 ± 5.78	6.43 ± 3.53	4.47 ± 2.29	9.18 ± 3.20	4.98 ± 3.76	4.14 ± 3.14	9.21 ± 4.90
SO_4^{2-} (μg m^{-3})	9.92 ± 3.70	8.89 ± 3.86	11.37 ± 3.29	8.96 ± 6.11	4.41 ± 2.68	15.34 ± 2.20	9.04 ± 5.15	7.41 ± 3.14	17.22 ± 6.50
Ca^{2+} (μg m^{-3})	2.19 ± 1.60	1.82 ± 1.35	2.69 ± 1.92	1.01 ± 0.51	1.05 ± 0.66	0.94 ± 0.19	1.71 ± 1.48	1.53 ± 1.52	2.60 ± 1.19
Mg^{2+} (μg m^{-3})	0.11 ± 0.06	0.09 ± 0.04	0.15 ± 0.07	0.05 ± 0.02	0.04 ± 0.01	0.06 ± 0.02	0.09 ± 0.08	0.06 ± 0.05	0.21 ± 0.05
NH_4^+ (μg m^{-3})	8.32 ± 3.04	7.36 ± 3.35	9.67 ± 2.16	4.88 ± 2.41	3.09 ± 0.90	7.40 ± 1.10	3.81 ± 2.53	3.05 ± 1.57	7.65 ± 3.61
nss-K^+ (μg m^{-3})	0.75 ± 0.29	0.62 ± 0.25	0.93 ± 0.25	0.76 ± 0.59	0.34 ± 0.33	1.35 ± 0.22	0.47 ± 0.40	0.33 ± 0.27	1.14 ± 0.25
nss-Cl^- (μg m^{-3})	1.61 ± 1.07	1.26 ± 1.04	2.10 ± 1.01	0.48 ± 0.43	0.64 ± 0.49	0.24 ± 0.17	0.17 ± 0.18	0.10 ± 0.06	0.51 ± 0.20
$C_8H_{17}O_4S^-$ (ng m^{-3})	0.26 ± 0.08	0.26 ± 0.10	0.27 ± 0.04	0.07 ± 0.05	0.09 ± 0.06	0.05 ± 0.02	0.08 ± 0.05	0.07 ± 0.03	0.13 ± 0.10

$C_5H_7O_6S^-$ (ng m^{-3})	4.60 ± 1.57	4.84 ± 1.90	4.27 ± 1.08	3.41 ± 0.70	3.42 ± 0.55	3.40 ± 0.94	3.22 ± 1.27	3.37 ± 1.32	2.49 ± 0.99
4NP (ng m^{-3})	2.53 ± 1.49	2.16 ± 1.73	3.05 ± 1.00	0.87 ± 0.43	0.79 ± 0.52	0.99 ± 0.25	1.62 ± 1.22	1.25 ± 0.91	3.48 ± 0.67
3M4NP (ng m^{-3})	0.26 ± 0.22	0.24 ± 0.27	0.28 ± 0.16	0.01 ± 0.01	0.01 ± 0.02	0 ± 0	0.21 ± 0.21	0.15 ± 0.16	0.50 ± 0.14
2M4NP (ng m^{-3})	0.43 ± 0.39	0.41 ± 0.48	0.47 ± 0.27	0.02 ± 0.05	0.04 ± 0.06	0 ± 0	0.28 ± 0.28	0.2 ± 0.22	0.68 ± 0.21
2,4DNP (ng m^{-3})	0.67 ± 1.02	0.51 ± 0.66	0.88 ± 1.45	0.25 ± 0.24	0.33 ± 0.28	0.12 ± 0.04	0.19 ± 0.07	0.18 ± 0.05	0.23 ± 0.15
Total NPs (ng m^{-3})	3.89 ± 2.88	3.33 ± 3.09	4.68 ± 2.66	1.15 ± 0.60	1.18 ± 0.78	1.12 ± 0.29	2.29 ± 1.70	1.77 ± 1.26	4.89 ± 1.16
4M5NC (ng m^{-3})	0.16 ± 0.03	0.15 ± 0	0.17 ± 0.05	0.16 ± 0.01	0.16 ± 0.02	0.16 ± 0	0.22 ± 0.13	0.20 ± 0.12	0.30 ± 0.19
4NC (ng m^{-3})	2.16 ± 1.23	2.04 ± 1.53	2.32 ± 0.76	3.28 ± 1.96	2.28 ± 1.79	4.67 ± 1.27	5.41 ± 3.82	4.09 ± 2.49	12.00 ± 0.60
Total NCs (ng m^{-3})	2.31 ± 1.22	2.19 ± 1.53	2.49 ± 0.72	3.44 ± 1.96	2.45 ± 1.79	4.83 ± 1.27	5.62 ± 3.89	4.29 ± 2.57	12.31 ± 0.41
5NSA (ng m^{-3})	0.43 ± 0.28	0.35 ± 0.29	0.54 ± 0.26	0.38 ± 0.31	0.22 ± 0.29	0.60 ± 0.16	0.19 ± 0.19	0.16 ± 0.20	0.31 ± 0.06
3NSA (ng m^{-3})	0.31 ± 0.23	0.26 ± 0.19	0.38 ± 0.28	0.17 ± 0.20	0.03 ± 0.07	0.37 ± 0.13	0.19 ± 0.20	0.16 ± 0.18	0.35 ± 0.33
Total NSAs (ng m^{-3})	0.74 ± 0.49	0.60 ± 0.46	0.92 ± 0.53	0.55 ± 0.47	0.25 ± 0.34	0.97 ± 0.24	0.37 ± 0.38	0.32 ± 0.37	0.66 ± 0.39
4NG (ng m^{-3})	0.39 ± 0.29	0.40 ± 0.38	0.36 ± 0.08	0.41 ± 0.28	0.37 ± 0.35	0.46 ± 0.14	0.75 ± 0.61	0.54 ± 0.39	1.83 ± 0.17
Total NACs (ng m^{-3})	7.33 ± 4.34	6.52 ± 5.23	8.45 ± 2.85	5.55 ± 2.75	4.24 ± 2.75	7.37 ± 1.53	9.04 ± 6.41	6.91 ± 4.44	19.69 ± 1.36

Table S5. Average contribution of secondarily formed NACs to the total measured NACs mass in $PM_{2.5}$ in different periods and locations.

Sites	Clean period	Polluted period	Average
HEB	91.96 ± 4.02 %	89.49 ± 3.32 %	90.93 ± 3.80 %
TY	87.62 ± 7.02 %	70.48 ± 7.35 %	80.48 ± 11.16 %
XA	94.38 ± 1.77 %	88.23 ± 3.46 %	91.82 ± 4.01 %
LZ	85.28 ± 4.24 %	79.25 ± 3.83 %	82.77 ± 4.98 %
BJ	90.99 ± 3.66 %	72.66 ± 7.59 %	86.41 ± 9.43 %
All northern cities	90.00 ± 3.16 %	80.20 ± 7.91 %	87.00 ± 4.59 %
CD	93.53 ± 4.73 %	95.39 ± 1.49 %	94.31 ± 3.73 %
KM	93.17 ± 4.54 %	95.24 ± 1.98 %	93.86 ± 3.90 %
WH	91.52 ± 4.00 %	93.02 ± 3.31 %	92.27 ± 3.59 %
HZ	91.52 ± 4.84 %	94.57 ± 2.17 %	92.79 ± 4.12 %
GZ	95.37 ± 4.80 %	97.99 ± 0.26 %	96.46 ± 3.80 %
GY	86.00 ± 9.23 %	96.81 ± 0.69 %	87.80 ± 9.35 %
All southern cities	92.00 ± 3.15 %	96.00 ± 1.57 %	93.00 ± 2.67 %

Figure S1.

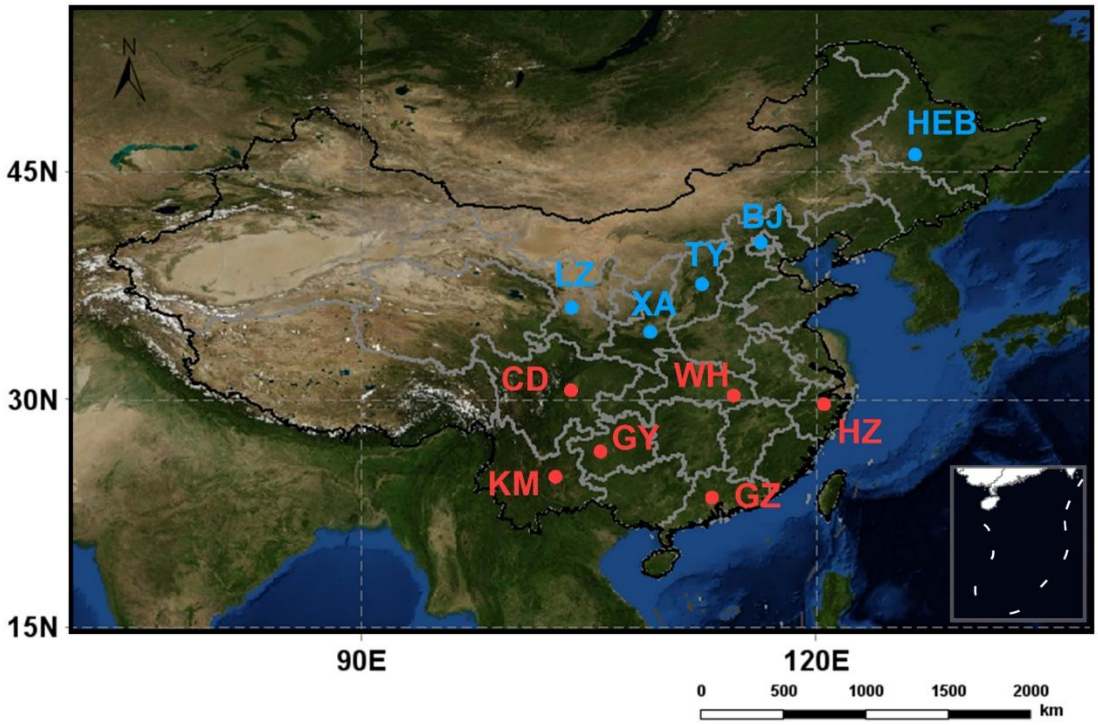

Figure S1. The locations of the sampling sites. The map was derived from ©MeteoInfoMap (Chinese Academy of Meteorological Sciences, China). The latitude and longitude of sampling sites are as follows: BJ (40.043°N, 116.412°E), LZ (36.106°N, 103.731°E), XA (34.249°N, 108.984°E), HEB (45.767°N, 126.635°E), TY (37.803°N, 112.584°E), KM (25.065°N, 102.696°E), GZ (23.180°N, 113.352°E), GY (26.651°N, 106.610°E), HZ (30.295°N, 20.165°E), CD (30.679°N, 104.142°E), and WH (30.546°N, 114.357°E). In the figure, the blue text labels represent northern cities, and the red text labels represent southern cities.

Figure S2.

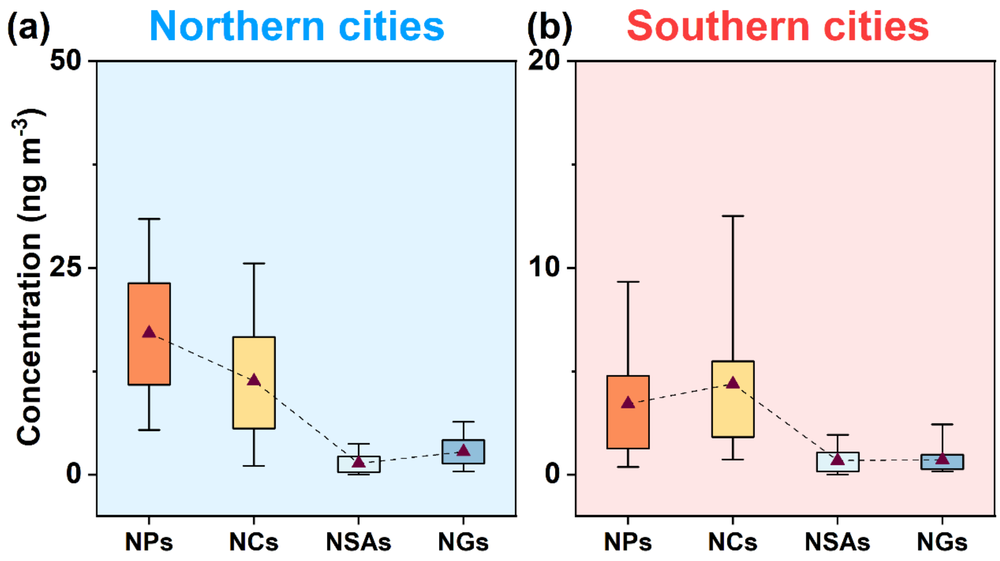

Figure S2. Box-and-whisker plots showing the variations in the concentration of different NAC groups in $PM_{2.5}$ for the pooled data from (a) northern and (b) southern cities. Each box encompasses the 25th–75th percentiles. The whiskers extend from the 5th to the 95th percentiles. The triangles inside boxes indicate the mean.

Figure S3.

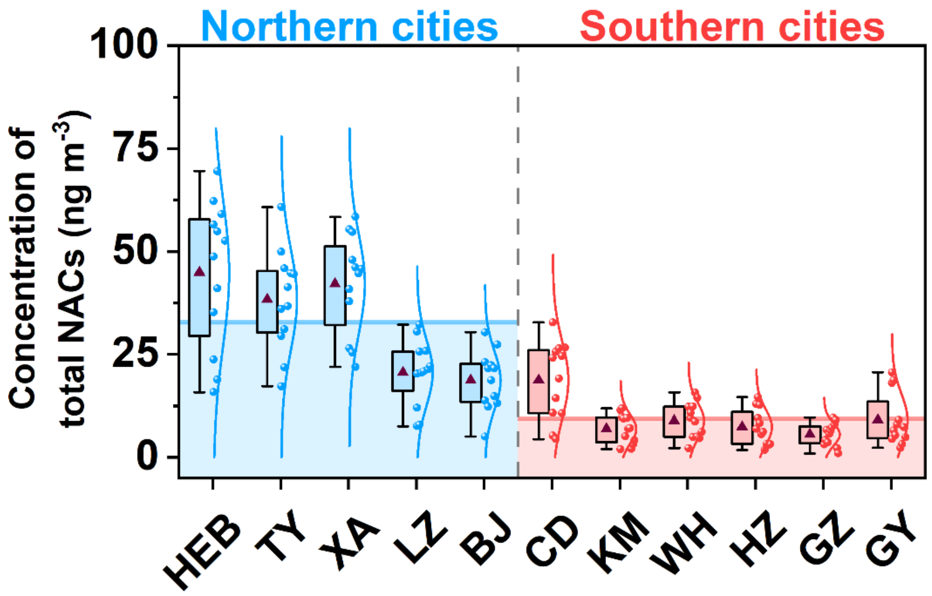

Figure S3. Box and whisker plots showing the variations in the mean concentrations of total NACs in $PM_{2.5}$ collected in 11 Chinese cities during winter. Each box encompasses the 25th–75th percentiles. The whiskers extend from the 5th to the 95th percentiles. The solid triangles inside boxes indicate the mean.

Figure S4.

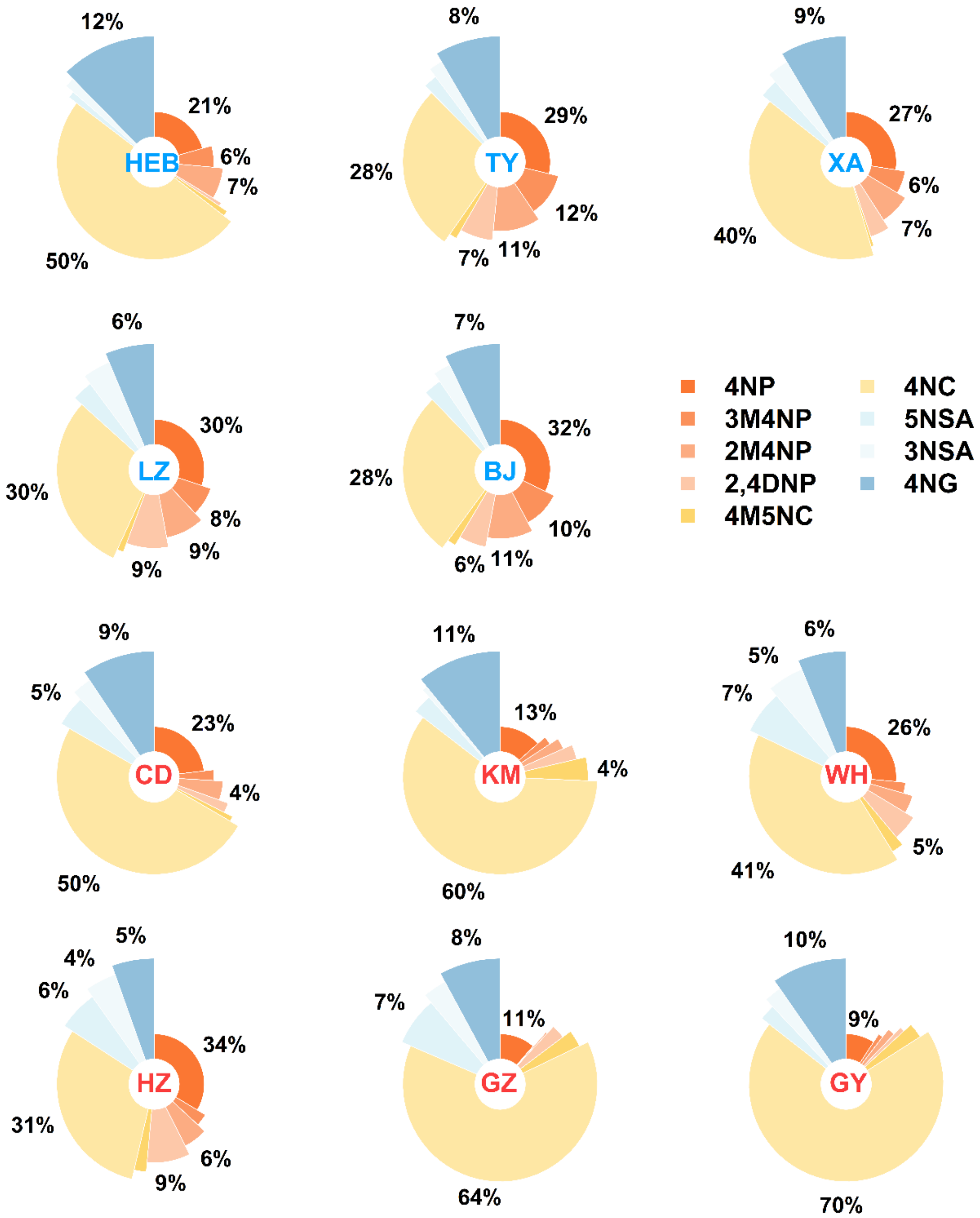

Figure S4. Average percentage distributions of various NAC species in $PM_{2.5}$ collected in 11 Chinese cities during winter.

Figure S5.

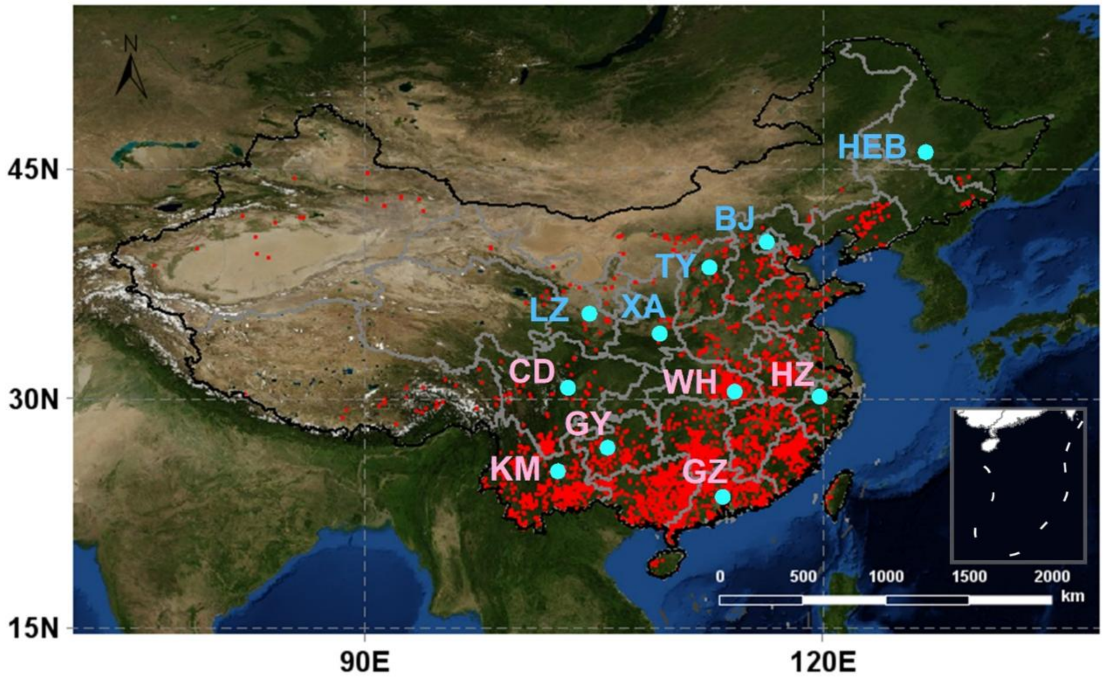

Figure S5. Spatial distribution of open fire spots in China during the sampling period (December 10, 2017 to January 14, 2018). The map was derived from ©MeteoInfoMap (Chinese Academy of Meteorological Sciences, China). In the figure, the blue text labels represent northern cities, and the pink text labels represent southern cities.

Figure S6.

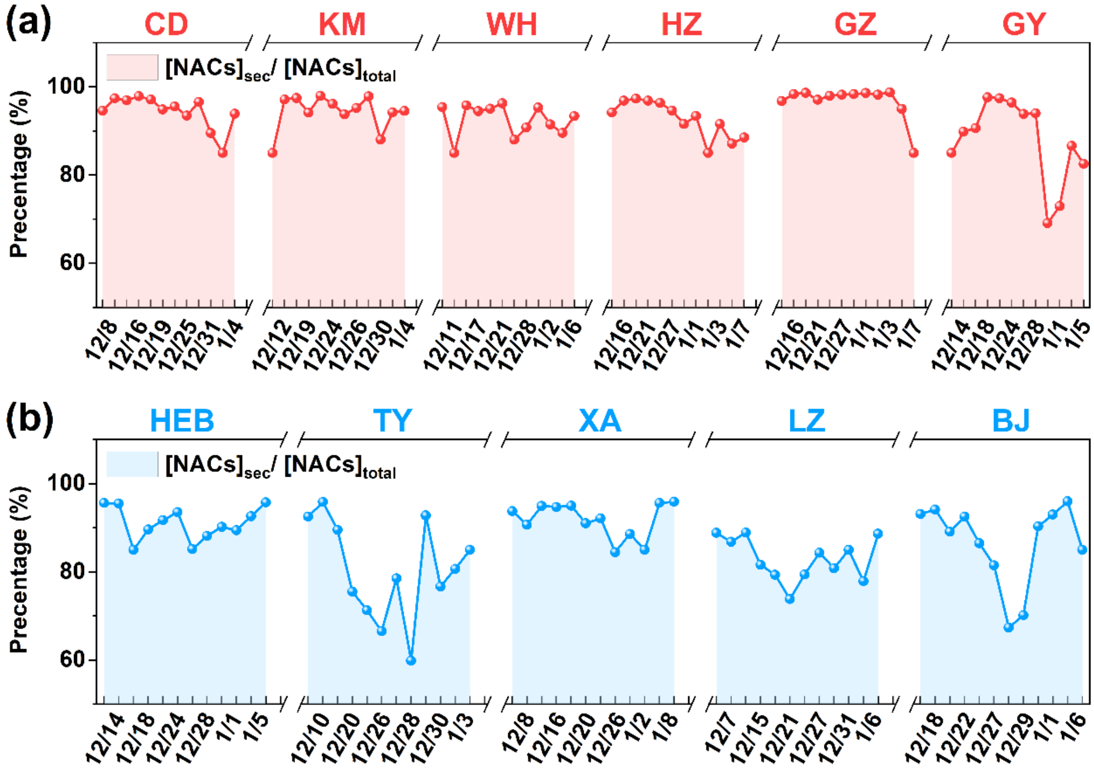

Figure S6. Temporal variations in the contribution of secondarily formed NACs to the total measured NACs mass in $PM_{2.5}$ in (a) southern and (b) northern cities.

Figure S7.

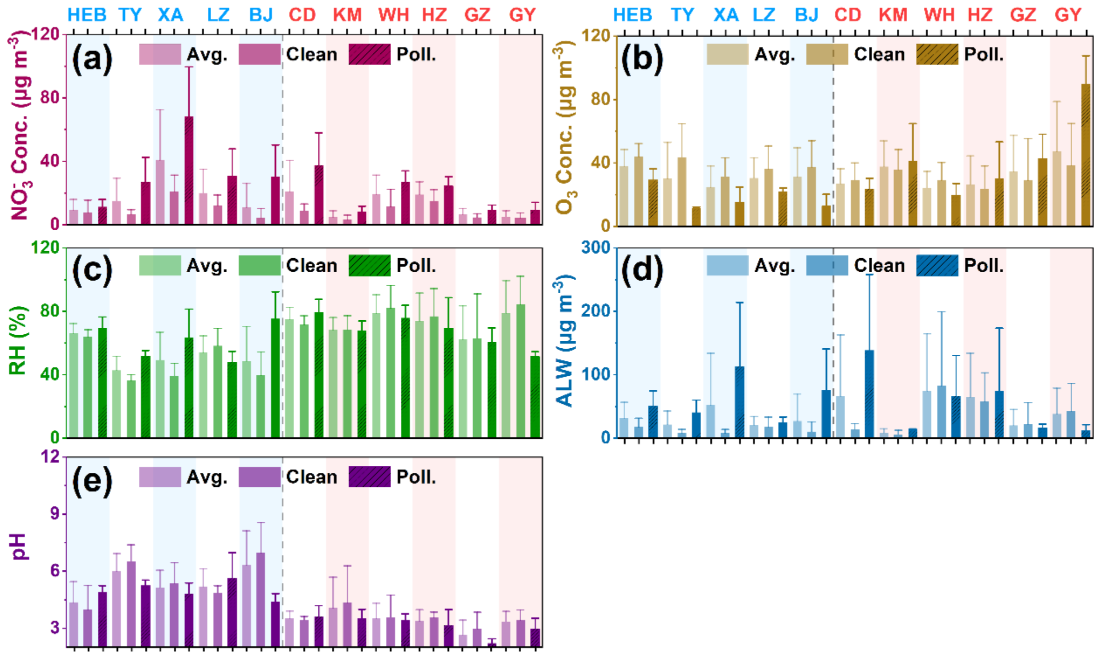

Figure S7. Average levels of (a) NO_3^-, (b) O_3, (c) RH, (d) ALW, and (e) pH across different periods in 11 Chinese cities.

References

Ding, J., Zhao, P., Su, J., Dong, Q., Du, X., and Zhang, Y.: Aerosol pH and its driving factors in Beijing, Atmos. Chem. Phys., 19, 7939-7954, 10.5194/acp-19-7939-2019, 2019.

Ehhalt, D. H. and Rohrer, F.: Dependence of the OH concentration on solar UV, J. Geophys. Res.: Atmos., 105, 3565-3571, 10.1029/1999jd901070, 2000.

Fountoukis, C. and Nenes, A.: ISORROPIA II: a computationally efficient thermodynamic equilibrium model for K+–Ca 2+–Mg 2+–NH 4+–Na+–SO 4 2−–NO 3−–Cl−–H 2 O aerosols, Atmos. Chem. Phys., 7, 4639-4659, 2007.

Guo, H. Y., Xu, L., Bougiatioti, A., Cerully, K. M., Capps, S. L., Hite Jr, J., Carlton, A., Lee, S. H., Bergin, M., and Ng, N.: Fine-particle water and pH in the southeastern United States, Atmos. Chem. Phys., 15, 5211-5228. https://doi.org/5210.5194/acp-5215-5211-2015, 2015.

He, Q. F., Ding, X., Fu, X. X., Zhang, Y. Q., Wang, J. Q., Liu, Y. X., Tang, M. J., Wang, X. M., and Rudich, Y.: Secondary Organic Aerosol Formation from Isoprene Epoxides in the Pearl River Delta, South China: IEPOX- and HMML-Derived Tracers, J. Geophys. Res.: Atmos., 123, 6999-7012, 2018.

Hofzumahaus, A., Rohrer, F., Lu, K., Bohn, B., Brauers, T., Chang, C.-C., Fuchs, H., Holland, F., Kita, K., Kondo, Y., Li, X., Lou, S., Shao, M., Zeng, L., Wahner, A., and Zhang, Y.: Amplified Trace Gas Removal in the Troposphere, Science, 324, 1702-1704, doi:10.1126/science.1164566, 2009.

Li, Z., Xue, L., Yang, X., Zha, Q., Tham, Y. J., Yan, C., Louie, P. K. K., Luk, C. W. Y., Wang, T., and Wang, W.: Oxidizing capacity of the rural atmosphere in Hong Kong, Southern China, Sci. Total Environ., 612, 1114-1122, 10.1016/j.scitotenv.2017.08.310, 2018.

Nguyen, T. K. V., Zhang, Q., Jimenez, J. L., Pike, M., and Carlton, A. G.: Liquid water: ubiquitous contributor to aerosol mass, Environ. Sci. Tech. Let., 3, 257-263. https://doi.org/210.1021/acs.estlett.1026b00167, 2016.

Nguyen, T. K. V., Petters, M., Suda, S., Guo, H., Weber, R., and Carlton, A.: Trends in particle-phase liquid water during the Southern Oxidant and Aerosol Study, Atmos. Chem. Phys., 14, 10911-10930. https://doi.org/10910.15194/acp-10914-10911-12014, 2014.

Song, S., Gao, M., Xu, W., Shao, J., Shi, G., Wang, S., Wang, Y., Sun, Y., and McElroy, M. B.: Fine-particle pH for Beijing winter haze as inferred from different thermodynamic equilibrium models, Atmos. Chem. Phys., 18, 7423-7438, 10.5194/acp-18-7423-2018, 2018.

Vaughan, S., Ingham, T., Whalley, L. K., Stone, D., Evans, M. J., Read, K. A., Lee, J. D., Moller, S. J., Carpenter, L. J., Lewis, A. C., Fleming, Z. L., and Heard, D. E.: Seasonal observations of OH and HO2 in the remote tropical marine boundary layer, Atmos. Chem. Phys., 12, 2149-2172, 10.5194/acp-12-2149-2012, 2012.

Wang, G., Jia, S., Li, R., Ma, S., Chen, X., Wu, Z., Shi, G., and Niu, X.: Seasonal variation characteristics of hydroxyl radical pollution and its potential formation mechanism during the daytime in Lanzhou, J. Environ. Sci., 95, 58-64, https://doi.org/10.1016/j.jes.2020.03.045, 2020.

Wang, Y., Hu, M., Hu, W., Zheng, J., Niu, H., Fang, X., Xu, N., Wu, Z., Guo, S., Wu, Y., Chen, W., Lu, S., Shao, M., Xie, S., Luo, B., and Zhang, Y.: Secondary Formation of Aerosols Under Typical High-Humidity Conditions in Wintertime Sichuan Basin, China: A Contrast to the North China Plain, J. Geophys. Res.: Atmos., 126, e2021JD034560, https://doi.org/10.1029/2021JD034560, 2021.

Xu, Y., Dong, X. N., He, C., Wu, D. S., Xiao, H. W., and Xiao, H. Y.: Mist cannon trucks can exacerbate the formation of water-soluble organic aerosol and PM2.5 pollution in the road environment, Atmos. Chem. Phys., 23, 6775-6788, 10.5194/acp-23-6775-2023, 2023.

Xu, Y., Miyazaki, Y., Tachibana, E., Sato, K., Ramasamy, S., Mochizuki, T., Sadanaga, Y., Nakashima, Y., Sakamoto, Y., Matsuda, K., and Kajii, Y.: Aerosol Liquid Water Promotes the Formation of Water-Soluble Organic Nitrogen in

Submicrometer Aerosols in a Suburban Forest, Environ. Sci. Technol., 54, 1406-1414. https://doi.org/1410.1021/acs.est.1409b05849, 2020.

Yan, C., Tham, Y. J., Zha, Q., Wang, X., Xue, L., Dai, J., Wang, Z., and Wang, T.: Fast heterogeneous loss of N2O5 leads to significant nighttime NOx removal and nitrate aerosol formation at a coastal background environment of southern China, Sci. Total Environ., 677, 637-647, https://doi.org/10.1016/j.scitotenv.2019.04.389, 2019.

Yang, T., Xu, Y., Ma, Y.-J., Wang, Y.-C., Yu, J. Z., Sun, Q.-B., Xiao, H.-W., Xiao, H.-Y., and Liu, C.-Q.: Field Evidence for Constraints of Nearly Dry and Weakly Acidic Aerosol Conditions on the Formation of Organosulfates, Environ. Sci. Technol. Lett., 11, 981-987, 10.1021/acs.estlett.4c00522, 2024.

Yin, M.-J., Xu, Y., Zhu, R.-G., Wang, Y., Sun, Q.-B., Gui, L., You, Y.-C., Tao, J.-L., Xiao, H.-W., Xiao, H., and Xiao, H.-Y.: Field New Insights into Bioaerosol Amino Acid Origin and Atmospheric Degradation: Significant Dust Contribution and Drying Effect, Environ. Sci. Technol., 60, 688-699, 10.1021/acs.est.5c12980, 2026.

You, Y.-C., Yang, T., Xu, Y., Gui, L., Wang, Y.-C., Yin, M.-J., Xiao, H., Xiao, H.-W., and Xiao, H.-Y.: Novel Discoveries about the Potential Nonsecondary Origins of C2–C3 Organosulfates in Ambient Aerosol Particles, Environ. Sci. Technol., 60, 6298-6309, 10.1021/acs.est.5c18511, 2026.